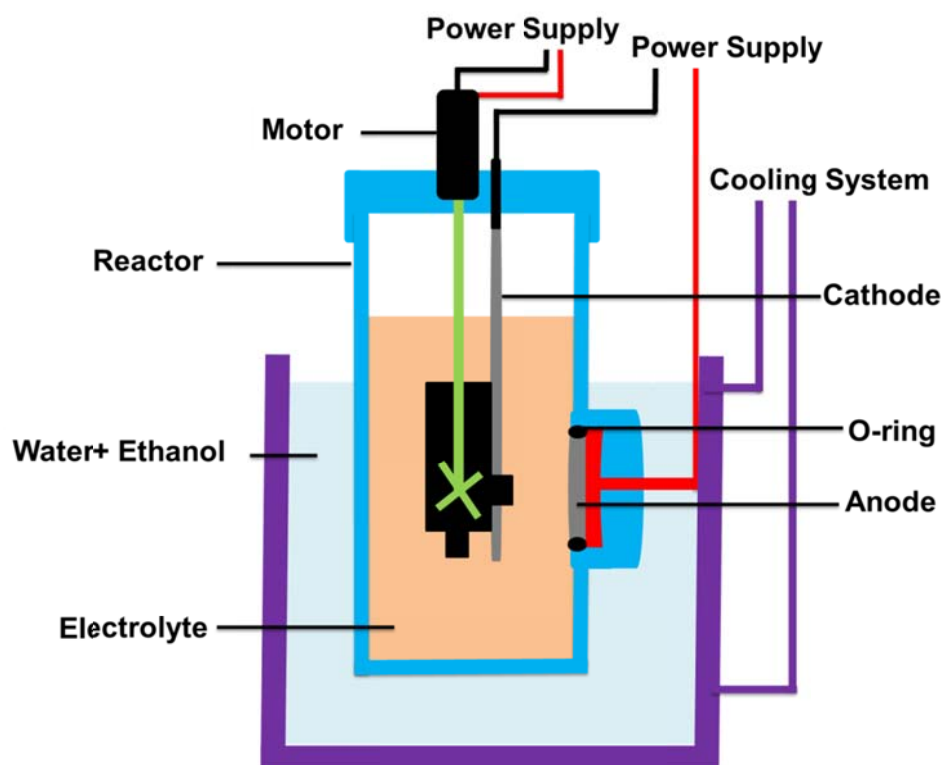


## Fabrication of Functional Polymeric Nanotubes with Modulated Pore Diameters

Mohammad Raoufi, Holger Schönherr\*

### Supporting Information



**Fig. S-1** Schematic of the reactor used for anodization. The temperature of the electrolyte in the reactor was adjusted by controlling the temperature of the cooling solution in the thermal reservoir during the anodization process. The central part is the electrolyte pump that was used to pump the electrolyte towards the anode with periodically changing flow rate. The cathode was fixed in front of the anode.

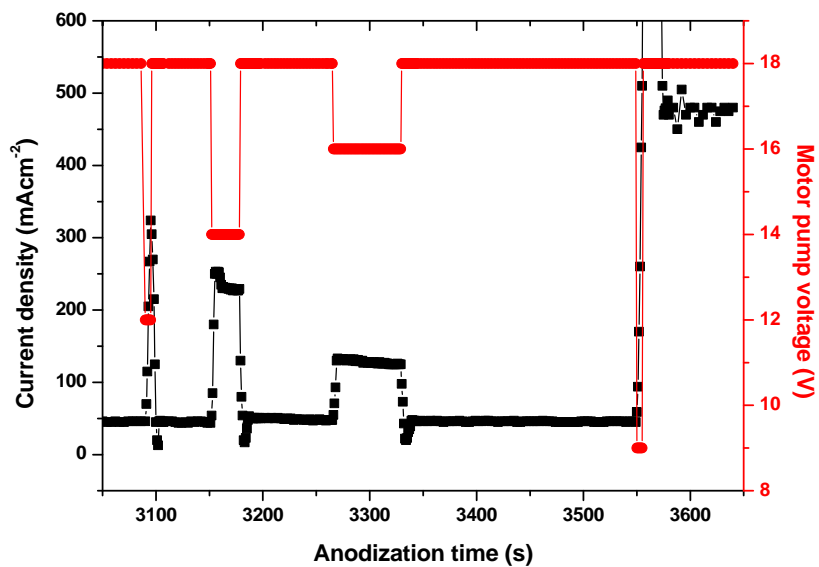


**Fig. S-2** Plot of current density and pump motor voltage as a function of time during temperature pulse anodization in a mixture of H<sub>2</sub>C<sub>2</sub>O<sub>4</sub> (0.3 M) and H<sub>3</sub>PO<sub>4</sub> (0.1 M) at 170 V.

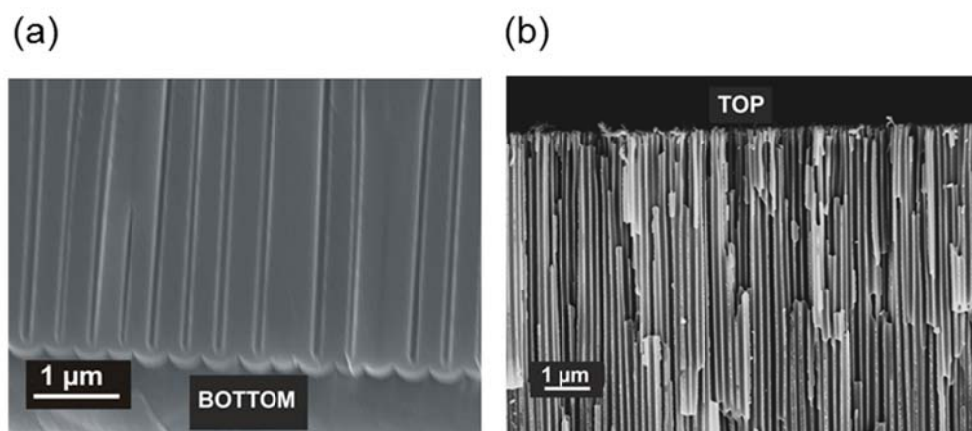


**Fig. S- 3** Cross-sectional FESEM images: (a) close-up views of the bottom side (barrier layer) and (b) the top side of diameter-modulated AAO fabricated by controlling the flow rate of the electrolyte during anodization in a mixture of  $\text{H}_3\text{PO}_4$  (0.3 M) and  $\text{H}_2\text{C}_2\text{O}_4$  (0.1M) at 170 V of the pores.

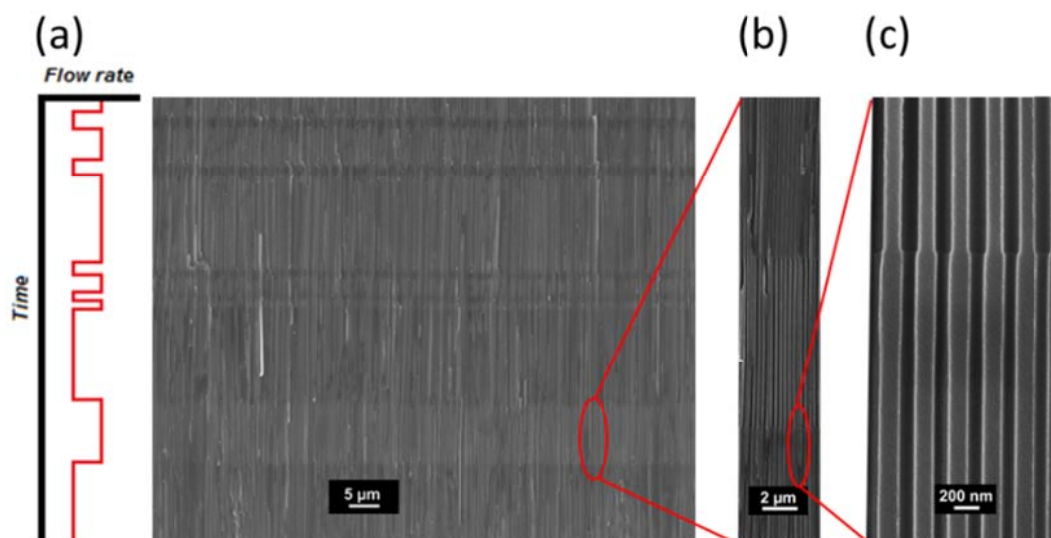


**Fig. S-4** Cross-sectional FESEM images: (a) Low-magnification and (b,c) high-magnification images of nanoporous AAO fabricated by controlling the flow rate of the electrolyte during HA in  $\text{H}_2\text{C}_2\text{O}_4$  (0.3 M) at 140 V. Different intervals of constant flow rate (2.0 s - 30 s) resulted different length of the segments with constant diameter (1.0 μm - 15.5 μm).

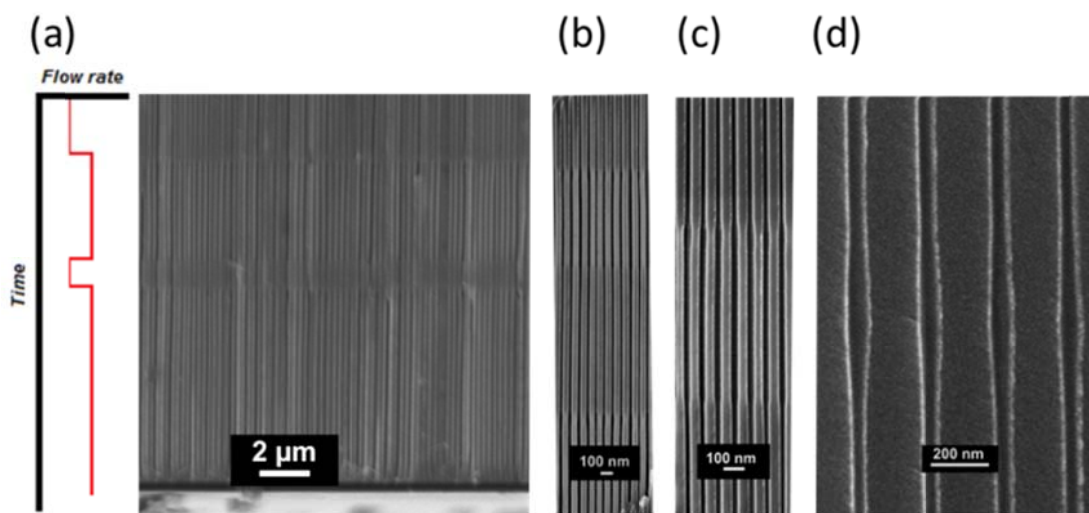


**Fig. S-5** (a) Low magnification and (b), (c) high magnification cross-sectional FESEM images of nanoporous AAO fabricated by controlling the flow rate of the electrolyte during HA in  $\text{H}_2\text{C}_2\text{O}_4$  (0.3M) at 140 V. The pore diameters were modulated between  $82 \pm 6$  nm and  $120 \pm 7$  nm. (d) FESEM image of nanopores with modulated diameter between  $40 \pm 3$  nm and  $65 \pm 4$  nm fabricated in  $\text{H}_2\text{C}_2\text{O}_4$  (0.3M) at 120 V. The interpore distances for 140 V and 120 V were  $273 \pm 6$  nm and  $234 \pm 9$  nm, respectively.

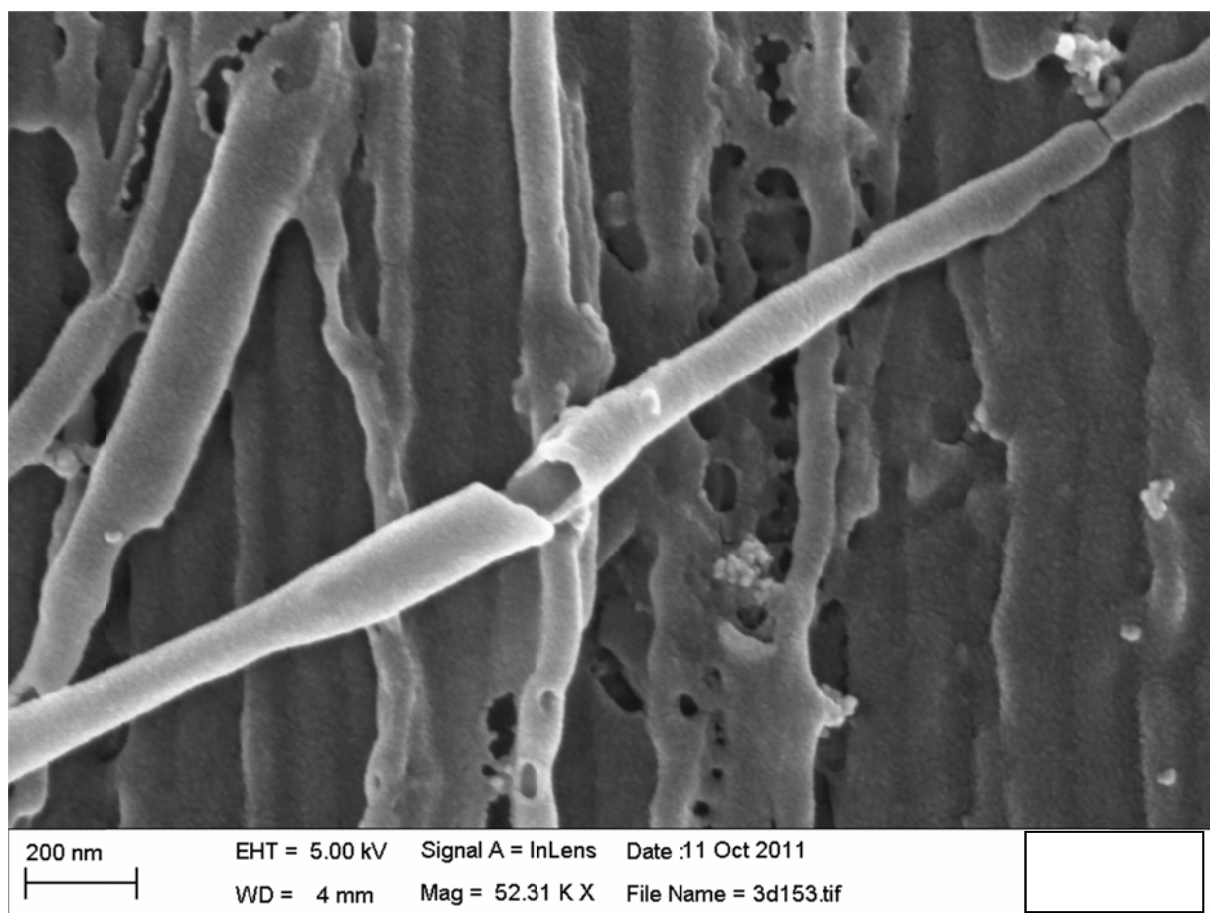


**Fig. S-6** FESEM images of broken nanotube. The wall thickness in the wide segment with a diameter of  $167 \pm 8$  nm is also  $\sim 10$  nm.

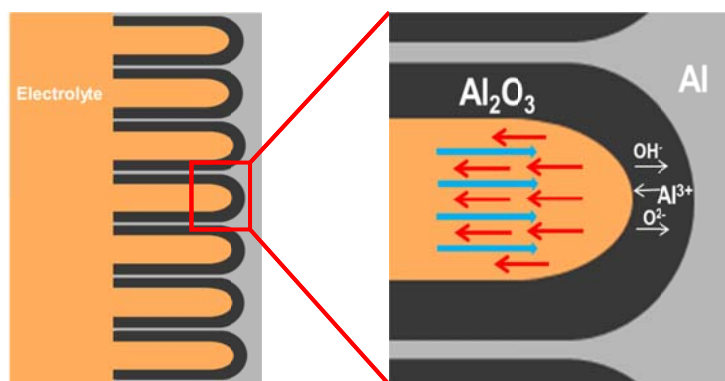


**Fig. S-7** Schematic of ion movement and aluminum oxide dissolution during the anodization process.

According to Joule's equation, the heat ( $q$ ) that is transferred in a given time is related to the square of the current density ( $J$ ), the barrier layer resistance ( $R$ ) and the time ( $t$ ).

$$q = R J^2 t \quad (\text{equation 1})$$

Reduced cooling results in less efficient dissipation of the heat that is liberated in the oxidation reaction. According to conductivity theory<sup>1</sup>, the high current density in HA is attributed to a reduction in barrier layer thickness with increasing voltage. High current densities were observed experimentally (Figures 2 and S-2), which is explained by the reduced resistance of barrier layer (thinner barrier layer). The high current density associated by periodic heating to barrier layer has also been reported to change the curvature of the barrier layer at the Al/Al<sub>2</sub>O<sub>3</sub> interfaces.<sup>2</sup> This periodic temperature change in the barrier layer could vary the detailed geometry of the barrier layer and hence the pore diameter.<sup>3,4</sup> In addition, the volume expansion factor involved in the oxidation process was reported to increase with current density.<sup>5</sup> Hence we may assume that the high current density will also generate a higher mechanical stress that aids the rapid oxide dissolution at the interface of Al and Al<sub>2</sub>O<sub>3</sub>.<sup>5,6</sup>

---

1 N. Cabrera and N. F. Mott, *Rep. Prog. Phys.*, 1949, **12**, 163–184.

2 W. Lee and J. C. Kim, *Nanotechnology*, 2010, **21**, 485304.

3 H. Asoh, K. Nishio, M. Nakao, A. Yokoo, T. Tamamura and H. Masuda, *J. Electrochem. Soc.*, 2001, **19**, 569–572.

4 S. Shingubara, K. Morimoto, H. Sakaue and T. Takahagi, *Electrochem. Solid-State Lett.*, 2004, **7**, E15–E17.

5 R. Krishnan and C. V. Thompson, *Adv. Mater.*, 2007, **19**, 988–992.

6 O. Jessensky, F. Müller and U. Gösele, *Appl. Phys. Lett.*, 1998, **72**, 1173–1175.